

INTEGRATED PHOTONICS

https://doi.org/10.1070/QEL17475

Generation of plasmon modes in a supernarrow nanoslit formed by silver surfaces

A.K. Sarychev, A.V. Ivanov, G. Barbillon

Abstract. **We report a theoretical study of plasmon generation of a giant electromagnetic field in a supernarrow nanoslit formed by a silver cylinder and a flat mirror surface. It is shown that as the silver surfaces approach each other, gap plasmons are excited in the gap between them, which results in a resonant amplification of the field. It is demonstrated for the first time that the electric field amplification increases with decreasing distance between the cylindrical and flat surfaces and reaches saturation, at which the field intensity becomes record high, exceeding the incident wave intensity by ten orders of magnitude. The found gap plasmon modes will increase the sensitivity to the detection of small concentrations of molecules, down to single molecules, by the methods of giant Raman scattering of light and plasmon-enhanced IR spectroscopy.**

Keywords: *plasmon resonance, nanoslit, slit plasmons, giant Raman scattering of light.*

1. Introduction

Surface-enhanced Raman scattering (SERS) is a promising method for highly sensitive probing of molecules [1–5]. SERS is extremely important for medical diagnostics, for example, for detecting pathologies in the body, including tumour formations; for optical imaging; and for quantitative detection of various biomarkers, including glycated proteins, cardiovascular biomarkers, etc. [6–10]. SERS has prospects for use in modern medical diagnostics in vivo in real time and in point-of-care diagnostics [11, 12]. In addition, it is possible to use the SERS effect in the field of environmental and food safety for the detection of pathogenic bacteria, viruses, bactericides, and toxins [13–15], as well as of ultra-low concentrations of nerve agents and explosives [16, 17]. Currently, the enhancement of the local electromagnetic field and the achievement of the SERS effect is provided by both periodically and chaotically located plasmonic nanoresonators in the form of wires, disks, holes, dimers of nanoparticles of various shapes, cones, tips, zigzag nanoslits, etc. [18–41]. Typical SERS gains vary from 10^4 to 10^9 for substrates consisting of clusters of gold or silver nanoparticles encapsulated in a dielectric matrix. Numerous theoretical predictions and experimental studies indicate the existence of giant fluctuations of the electromagnetic field in almost contacting plasmonic nanoparticles near the percolation threshold [42–49]. Plasmonic nanoslits play a special role in strengthening the local plasmon field.

In recent years, there have been many works devoted to almost contacting particles with gaps several nanometers thick [50–67]. In [41, 51, 52], an enhanced field was generated in a supernarrow nanoslit formed by a gold nanoparticle placed on a gold mirror. The evolution of various gap plasmons with a change in the gap thickness from 1 to 5 nm has been considered. It has been shown that when the thickness of the gap and the shape of the nanoparticles change from sphere to cube, the coupling of transverse waveguide and so-called antenna modes changes, which leads to the appearance of hybridised plasmons covering the entire nanoparticle.

In this work, we theoretically investigated the generation of giant electromagnetic fields in a supernarrow plasmon nanoslit formed by smooth and cylindrical silver surfaces when the surfaces approach, almost up to their contact.

2. Supernarrow nanoslit formed by silver surfaces

The effect of plasmon generation of electromagnetic fields on nanometre scales seems to be very promising for the fabrication of new optical devices, in particular, for subnanometre probing of molecules. Controllable metamaterials based on plasmonic nanoresonators make it possible to excite amplified electromagnetic fields at certain frequencies by specifying the geometry and spatial arrangement of nanoresonators. In this work, we investigate the generation of giant electromagnetic fields in a supernarrow nanoslit formed by smooth and cylindrical silver surfaces (Fig. 1).

Resonance modes in such a slit resonator can be obtained in the quasi-static approximation by solving the Laplace equation, since it is assumed that the gap thickness d is much less than the wavelength of electromagnetic radiation. The electric field excited by the incident radiation in the gap between the cylinder and the metal surface is decomposed into gap modes and can be calculated analytically.

To find the distribution of the electric field strength, we use the conformal mapping method:

$$w = u + \mathrm{i}v = \ln[(l + x + \mathrm{i}y)(l - x - \mathrm{i}y)], \quad (1)$$

where $l = \sqrt{d(2a + d)}$ is the size of the region of plasmon localisation in the gap ($d \ll l \ll a$). Conformal mapping (1) transforms the xy plane into the region $0 < v < 2\pi$. The right edge of this region ($u > u_1$, $u_1 = \ln[(l + d)/(l - d)]$ is a cylinder,

A.K. Sarychev, A.V. Ivanov Institute for Theoretical and Applied Electromagnetics, Russian Academy of Sciences, ul. Izhorskaya 13, 125412 Moscow, Russia; e-mail: sarychev_andrey@yahoo.com
G. Barbillon EPF-Ecole d'Ingénieurs, 3 bis rue Lakanal, 92330 Sceaux, France

Received 5 November 2020
Kvantovaya Elektronika **51** (1) 79–83 (2021)
Translated by I.A. Ulitkin

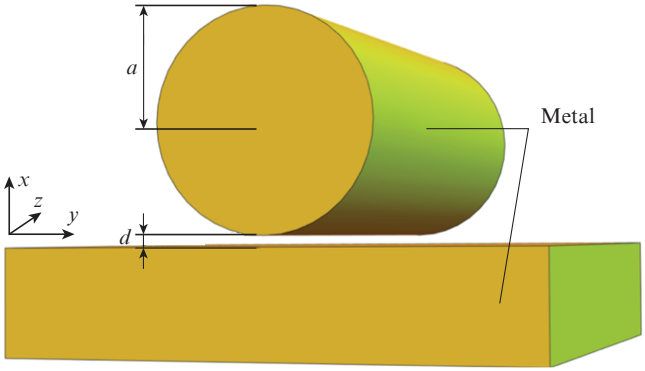

Figure 1. Silver cylinder near a smooth silver surface.

and the left edge ($u < 0$) is a plane. The space between them ($0 < u < u_1$) is a gap and plays the role of capacitance, while the cylinder and the plane play the role of inductance. The complex potentials in these regions have the form

$$\varphi^{\mathrm{L}} = \varphi_0 + \sum_{q=1}^{\infty} [B_3^{(q)} f_{\mathrm{Lc}}^{(q)} + B_4^{(q)} f_{\mathrm{Ls}}^{(q)}], \quad u < 0, \tag{2}$$

$$\varphi^{\mathrm{R}} = \varphi_0 + \sum_{q=1}^{\infty} [B_1^{(q)} f_{\mathrm{Rc}}^{(q)} + B_2^{(q)} f_{\mathrm{Rs}}^{(q)}], \quad u > u_1, \tag{3}$$

$$\varphi^{\mathrm{G}} = \varphi_0 + \sum_{q=1}^{\infty} [A_1^{(q)} f_{\mathrm{Rc}}^{(q)} + A_2^{(q)} f_{\mathrm{Rs}}^{(q)} + A_3^{(q)} f_{\mathrm{Lc}}^{(q)} + A_4^{(q)} f_{\mathrm{Ls}}^{(q)}], \quad 0 < u < u_1, \tag{4}$$

where

$$f_{\mathrm{Rc}}^{(q)} = \exp(-qu)\cos qv;$$

$$f_{\mathrm{Rs}}^{(q)} = \exp(-qu)\sin qv;$$

$$f_{\mathrm{Lc}}^{(q)} = \exp(qu)\cos qv;$$

$$f_{\mathrm{Ls}}^{(q)} = \exp(qu)\sin qv.$$

The electric field is set in a standard way: $E_u = -\partial\varphi/\partial u$ and $E_v = -\partial\varphi/\partial v$. Next, we will find the coefficients in equations (2)–(4) using the boundary conditions for the electric field. These boundary conditions are the continuity of the tangential component of the electric field and the continuity of the normal component of the electric displacement. Coefficients $A_1^{(q)}$, $A_2^{(q)}$, $A_3^{(q)}$, $A_4^{(q)}$, $B_1^{(q)}$, $B_2^{(q)}$, $B_3^{(q)}$, and $B_4^{(q)}$ are determined from these conditions:

$$E_v^{\mathrm{R}} = E_v^{\mathrm{G}}, \ \varepsilon_{\mathrm{m}} E_u^{\mathrm{R}} = \varepsilon_{\mathrm{d}} E_u^{\mathrm{G}} \quad \text{for } u = u_1, \tag{5}$$

$$E_v^{\mathrm{L}} = E_v^{\mathrm{G}}, \ \varepsilon_{\mathrm{m1}} E_u^{\mathrm{L}} = \varepsilon_{\mathrm{d}} E_u^{\mathrm{G}} \quad \text{for } u = 0, \tag{6}$$

where ε_{d} is the permittivity in the gap; and ε_{m} and $\varepsilon_{\mathrm{m1}}$ are dielectric constants of the plane and cylinder, respectively. Zeroing the determinant of linear equations for the qth coefficients $A_i^{(q)}$ and $B_i^{(q)}$ ($i = 1$–4) leads to the dispersion equation for resonant frequencies, i.e. for the frequencies of gap plasmons:

$$g_1^{2q}[\varepsilon_{\mathrm{d}} + \varepsilon_{\mathrm{m}}(\omega)][\varepsilon_{\mathrm{d}} + \varepsilon_{m1}(\omega)] + [\varepsilon_{\mathrm{m}}(\omega) - \varepsilon_{\mathrm{d}}][\varepsilon_{\mathrm{d}} - \varepsilon_{m1}(\omega)] = 0, \tag{7}$$

where $g_1 = (l + d)/(l - d)$. The electric field obtained in this way depends on the wavelength, the angle of incidence of the light, and the ratio of the gap thickness d to the cylinder radius a. In a narrow slit, $d \ll a$, the field is concentrated on the spatial scale $l \propto \sqrt{ad}$ ($d \ll l \ll a$) and oscillates depending on the ratio d/a. The field maxima arise when an integer number of gap modes fits on the scale l.

Analytical calculations were performed for an electric field localised in a gap between a metal cylinder and a flat metal or semiconductor surface, and a system of periodically located cylinders was selected for numerical calculations. Numerical calculations were performed for a periodic system, since such a formulation of the problem is more consistent with a real experiment. It is assumed that a monomolecular layer of an active SERS-substance is located in the gaps formed by a periodic system of silver cylinders and a flat silver surface. In a real experiment, we expect record values of the SERS signal from single molecules located in such nanoslits. The results of the developed analytical theory for one nanoslit are in good agreement with the results of a numerical experiment performed using the COMSOL software package by solving the full system of Maxwell's equations. The good agreement between theory and numerical experiment is not accidental, since the electric field is localised in nanogaps, and, therefore, in the first approximation, the interaction between the cylinders can be neglected. The theory makes it possible to analytically calculate the field amplification for various combinations of nanocylinder materials and a smooth substrate. Thus, the developed analytical theory makes it possible to carry out the preliminary design of effective SERS sensors.

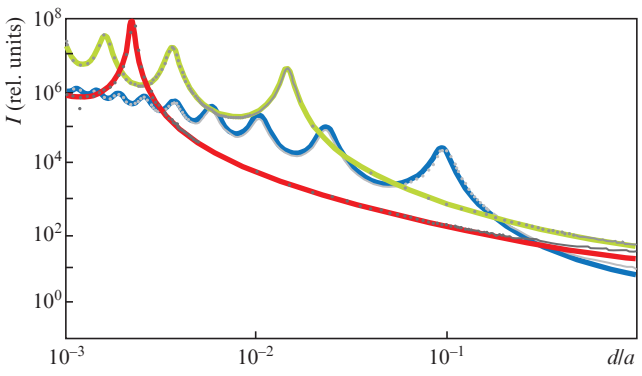

Figure 2. (Colour online) Relative intensity of the electric field as a function of the ratio of the slit width d to the cylinder radius a at $a = 4$ nm and the period of the cylinder arrangement $D = 531$ nm. Blue, green, and red curves correspond to $\lambda = 405$, 532 and 785 nm, respectively. The angle of incidence of the light is $\alpha = 45°$ with respect to the normal; the electromagnetic wave is p-polarised. The dots are the results of numerical calculations, which differ only slightly from the analytical results for $d/a > 1$.

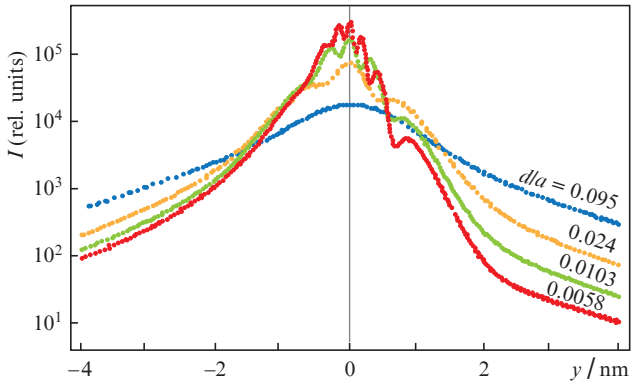

Figure 3. (Colour online) Spatial distributions of the electric field intensity in the slit on a scale of one cylinder with a radius $a = 4$ nm for the first four resonances at $\lambda = 405$ nm and an angle of incidence of the light, $a = 45°$.

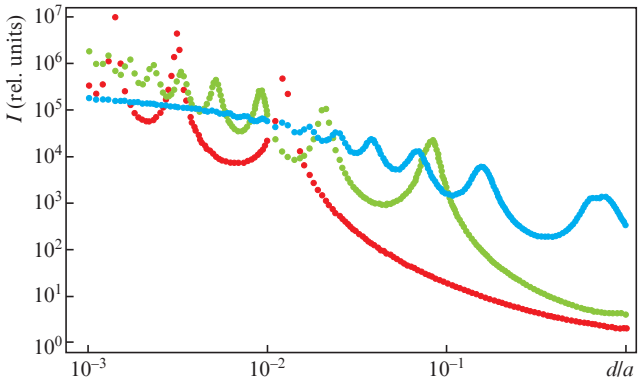

Figure 5. Relative intensity of the electric field as a function of the ratio d/a at $a = 4$ nm, $D = 300$ nm and the refractive index of the layer in the slit, $n = 1.534$. Blue, green and red dependences correspond to $\lambda = 405$, 532 and 785 nm, respectively. The angle of incidence of radiation is $\alpha = 45°$; the electromagnetic wave is p-polarised.

In comparing analytical and numerical results, use is made of the dielectric constant of silver, taken from the experimental data [68]. Figure 2 shows analytically and numerically calculated dependences of the electric field amplification in the slit on the ratio of the gap width d formed by two surfaces to the cylinder radius a. The calculations were performed for laser wavelengths $\lambda = 405$, 532, and 785 nm, which are often used in Raman spectroscopy.

In the quasi-static approximation ($\lambda \gg a$), the results of analytical and numerical calculations coincide with high accuracy. Figure 3 shows the evolution of the spatial distribution of the field in the slit for the first four resonances at $\lambda = 405$ nm. It can be seen that the number of field maxima in the slit on the scale of one cylinder increases with increasing d/a ratio. Figure 4 shows the results of numerical calculations of the reflection of an electromagnetic wave and the amplification of the electric field in a system of noninteracting cylinders for a wide range of wavelengths. It can be seen that the maximum of the field amplification corresponds to the reflection minimum. A nanoslit formed by a silver cylinder and a surface can be used to probe molecules. We place a dielectric layer with a refractive index $n = 1.534$ between the cylinder and the surface, simulating a molecular layer. The numerically calculated intensity of the electric field in this case is shown in Fig. 5. An additional dielectric layer leads to a shift in all resonances to the red region of the spectrum. This circumstance simplifies the experimental implementation of the effect under consideration.

3. Conclusions

Thus, we have investigated the plasmon field excited by laser radiation in a nanoslit between a metal cylinder and a metal mirror surface. It is shown that, as the nanoslit width decreases, the resonant field amplification in the gap between the surfaces increases up to saturation, at which plasmon modes begin to merge in the gap (this is clearly seen in Figs 2 and 3 at $\lambda = 405$ nm). The intensity of the electric field in the slit upon saturation increases by more than 10^6 times at $\lambda = 405$ nm, more than 10^8 times at $\lambda = 532$ nm, and more than

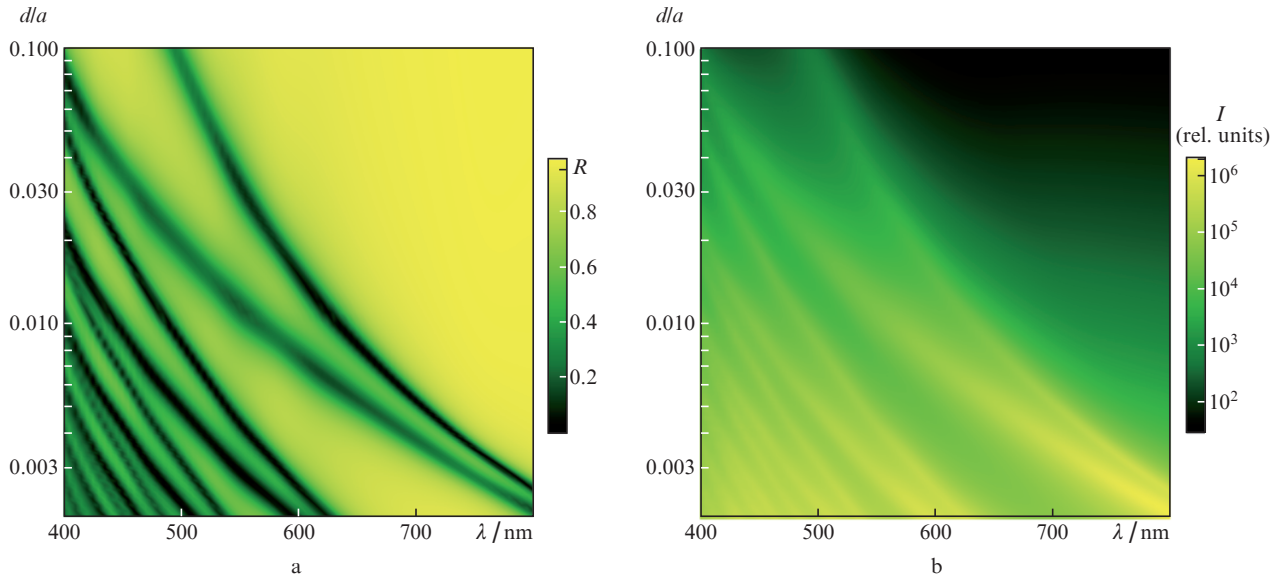

Figure 4. (Colour online) (a) Reflection coefficient and (b) relative intensity of the electric field as functions of the ratio d/a at $a = 50$ nm and period $D = 200$ nm.

10^9 times at $\lambda = 785$ nm compared to the intensity of the incident wave.

Placing a molecular layer with a refractive index $n = 1.534$ in a nanoslit leads to a red shift of the resonances. The resulting enhancement of the electric field reaches record values, which makes it possible to register low concentrations of molecules by the SERS method and other spectral methods. The considered slit resonators with a controllable slit thickness can be used to produce bound plasmon states and vibrations of molecules placed in the gap. The detection and study of such a hybrid state will make it possible to evaluate and understand many features of SERS and other plasmon effects.

Acknowledgements. This work was supported by the Russian Foundation for Basic Research (Grant No. 20-21-00080) and the Russian Science Foundation (Grant No. 16-14-00-209).

References

1. Zong C., Xu M., Xu L.-J., Wei T., Ma X., Zheng X.-S., Hu R., Ren B. *Chem. Rev.*, **118**, 4946 (2018).
2. Ding S.-Y., Yi J., Li J.-F., Ren B., Wu D.-Y., Panneerselvam R., Tian Z.-Q. *Nat. Rev.*, **1**, 1 (2016).
3. Ding S.-Y., You E.-M., Tian Z.-Q., Moskovits M. *Chem. Soc. Rev.*, **46**, 4042 (2017).
4. Itoh T., Yamamoto Y.S., Ozaki Y. *Chem. Soc. Rev.*, **46**, 3904 (2017).
5. Sharma B., Frontiera R.R., Henry A.-I., Ringe E., Van Duyne R.P. *Mater. Today*, **15**, 16 (2012).
6. Kneipp J. *ACS Nano*, **11**, 1136 (2017).
7. Hu Y., Cheng H., Zhao X., Wu J., Muhammad F., Lin S., He J., Zhou L., Zhang C., Deng Y., Wang P., Zhou Z., Nie S., Wei H. *ACS Nano*, **11**, 5558 (2017).
8. Andreou C., Neuschmelting V., Tschaharganeh D.-F., Huang C.-H., Oseledchyk A., Iacono P., Karabeber H., Colen R.R., Mannelli L., Lowe S.W., Kircher M.F. *ACS Nano*, **10**, 5015 (2016).
9. Nechaeva N.L., Boginskaya I.A., Ivanov A.V., Sarychev A.K., Eremenko A.V., Ryzhikov I.A., Lagarkov A.N., Kurochkin I.N. *Anal. Chim. Acta*, **1100**, 250 (2020).
10. Chon H., Lee S., Yoon S.-Y., Lee E.K., Chang S.-l., Choo J. *Chem. Commun.*, **50**, 1058 (2014).
11. Laing S., Jamieson L.E., Faulds K., Graham D. *Nat. Rev. Chem.*, **1**, 1 (2017).
12. Maiti K.K., Dinish U.S., Samanta A., Vendrell M., Soh K.-S., Park S.-J., Olivo M., Chang Y.-T. *Nano Today*, **7**, 85 (2012).
13. Liu Y., Zhou H., Hu Z., Yu G., Yang D., Zhao J. *Biosens. Bioelectron.*, **94**, 131 (2017).
14. Yang T., Zhang Z., Zhao B., Hou R.-Y., Kinchla A., Clark J.M., He L. *Anal. Chem.*, **88**, 5243 (2016).
15. Durmanov N., Guliev R.R., Eremenko A.V., Boginskaya I.A., Ryzhikov I.A., Trifonova E.A., Putlyaev E.V., Kalnov S.L., Balandina M.V., Tkachuk A.P., Gushchin V.A., Sarychev A.K., Lagarkov A.N., Rodionov I.A., Gabidullin A.R., Kurochkin I.N. *Sens. Actuators, B*, **257**, 37 (2018).
16. Chen N., Ding P., Shi Y., Jin T., Su Y., Wang H., He Y. *Anal. Chem.*, **89**, 5072 (2017).
17. Hakonen A., Rindcevicius T., Schmidt M.S., Andresson P.O., Juhlin L., Svedendahl M., Boisen A., Kall M. *Nanoscale*, **8**, 1305 (2016).
18. Zhang Y., Wang G., Yang L., Wang F., Liu A. *Coord. Chem. Rev.*, **370**, 1 (2018).
19. Qiao P., Yang W., Chang-Hasnain C.J. *Adv. Opt. Photonics*, **10**, 180 (2018).
20. Xavier J., Vincent S., Meder F., Vollmer F. *Nanophotonics*, **7**, 1 (2018).
21. Bandarenka H.V., Girel K.V., Bondarenko V.P., Khodasevich I.A., Panarin A.Y., Terekhov S.N. *Nanoscale Res. Lett.*, **11**, 262 (2016).
22. Kukushkin V.I., Grishina Ya.V., Solov'ev V.V., Kukushkin I.V. *JETP Lett.*, **105**, 677 (2017) [*Pis'ma Zh. Eksp. Teor. Fiz.*, **105**, 637 (2017)].
23. Fedotova Ya.V., Kukushkin V.I., Solovyev V.V., Kukushkin I.V. *Opt. Express*, **27**, 32578 (2019).
24. Barbillon G., Ivanov A., Sarychev A.K. *Nanomaterials*, **9**, 1 (2019).
25. Sarychev A.K., Ivanov A., Lagarkov A., Barbillon G. *Materials*, **12**, 103 (2019).
26. Barbillon G., Ivanov A., Sarychev A.K. *Symmetry*, **12**, 896 (2020).
27. Ivanov A., Sarychev A.K., Bykov I., Boginskaya I., Lagarkov A., Ryzhikov I., Nechaeva N., Kurochkin I. *J. Phys. Conf. Ser.*, **1461**, 012057 (2020).
28. Barbillon G. *Coatings*, **9**, 86 (2019).
29. Lee H.K., Lee Y.H., Koh C., Phan-Quang G.C., Han X., Lay C.L., Sim H.Y.F., Kao Y.-C., An Q., Ling X. *Chem. Soc. Rev.*, **48**, 731 (2019).
30. Hong Y., Pourmand M., Boriskina S.V., Reinhard B.M. *Adv. Mater.*, **25**, 115 (2013).
31. Gu P., Zhou Z., Zhao Z., Mohwald H., Li C., Chiechi R.C., Shi Z., Zhang G. *Nanoscale*, **11**, 3583 (2019).
32. Lagarkov A., Boginkaya I., Bykov I., Budashov I., Ivanov A., Kurochkin I., Ryzhikov I., Rodionov I., Sedova M., Zverev A., Sarychev A.K. *Opt. Express*, **25**, 17021 (2017).
33. Lagarkov A., Budashov I., Chistyaev V., Ezhov A., Fedyanin A., Ivanov A., Kurochkin I., Kosolobov S., Latyshev A., Nasimov D., Ryzhikov I., Shcherbakov M., Vaskin A., Sarychev A.K. *Opt. Express*, **24**, 7133 (2016).
34. Lee H.K., Lee Y.H., Lin Koh C.S., et al. *Chem. Soc. Rev.*, **48**, 731 (2018).
35. Lyu S., Lei D.Y., Liu W., Yao H., Mo D., Chen Y., Hu P., Sun Y., Liu J., Duan J.L. *RSC Advances*, **5**, 32103 (2015).
36. Matricardi C., Hanske C., Garcia-Pomar J.L., Langer J., Mihi A., Liz-Marzan L.M. *ACS Nano*, **12**, 8531 (2018).
37. Su J., Wang D., Norbel L., Shen J., Zhao Z., Dou Y., Peng T., Shi J., Mathur S., Fan C., Song S. *Anal. Chem.*, **89**, 2531 (2017).
38. Yan X., Wang M., Sun X., Wang Y., Shi G., Ma W., Hou P. *Appl. Surf. Sci.*, **479**, 879 (2019).
39. Zhang J., Li J., Tang S., Fang Y., Wang J., Huang G., Liu R., Zheng L., Cui X., Mei Y. *Sci. Rep.*, **5**, 1 (2015).
40. Yoon J.H., Selbach F., Langolf L., Schlucker S. *Small*, **14**, 1702754 (2018).
41. Wang X., Bai X., Pang Z., Yang H., Qi Y. *Results Phys.*, **12**, 1866 (2019).
42. Kuttner C., Mayer M., Dulle M., Moscoso A., Lopez-Romero J.M., Forster S., Fery A., Perez-Juste J., Contreras-Caceres R. *ACS Appl. Mater. Interfaces*, **10**, 11152 (2018).
43. Demetriadou A., Hamm J.M., Luo Y., Pendry J.B., Baumberg J.J., Hess O. *ACS Photonics*, **4**, 2410 (2017).
44. Ivanov A., Shalygin A., Lebedev V., Vorobev V., Vergiles S., Sarychev A.K. *Appl. Phys. A*, **107**, 17 (2012).
45. Frumin L.L., Nemykin A.V., Perminov S.V., Shapiro D.A. *J. Opt.*, **30**, 2048 (2013).
46. Liu Z.-Q., Liu G.-Q., Liu X.-S., Huang K., Chen Y.-H., Hu Y., Fu G.L. *Plasmonics*, **8**, 1285 (2013).
47. Liu G.-Q., Hu Y., Liu Z.-Q., Chen Y.-H., Cai Z.-J., Zhang X.-N., Huang K. *Phys. Chem. Chem. Phys.*, **16**, 4320 (2014).
48. Liu G.-Q., Hu Y., Liu Z.-Q., Cai Z.-J., Zhang X.-N., Chen Y.-H., Huang K. *Opt. Commun.*, **316**, 111 (2014).
49. Rasskazov I.L., Markel' V.A., Karpov S.V. *Opt. Spectrosc.*, **115**, 666 (2013) [*Opt. Spektrosk.*, **115**, 753 (2013)].
50. Seal K., Sarychev A.K., Noh H., Genov D.A., Yamilov A., Shalaev V.M., Ying Z.C., Cao H. *Phys. Rev. Lett.*, **94**, 226101 (2005).
51. Genov D., Shalaev V., Sarychev A. *Phys. Rev. B*, **72**, 113102 (2005).
52. Cai H., Wu Y., Dai Y., Pan N., Tian Y., Luo Y., Wang X. *Opt. Express*, **24**, 20808 (2016).
53. Chikkaraddy R., Zheng X., Benz F., Brooks L.J., de Nijs B., Carnegie C., Kleemann M.-E., Mertens J., Bowman R.W., Vandenbosch G., Moshchalkov V.V., Baumberg J.J. *ACS Photonics*, **4**, 469 (2017).
54. Chikkaraddy R., Turek V.A., Kongsuwan N., Benz F., Carnegie C., van de Goor T., de Nijs B., Demetriadou A., Hess O., Keyser U.F., Baumberg J.J. *Nano Lett.*, **18**, 405 (2018).
55. Fu Q., Zhan Z., Dou J., Zheng X., Xu R., Wu M., Lei Y. *ACS Appl. Mater. Interfaces*, **7**, 13322 (2015).

56. Jiang T., Chen G., Tian X., Tang S., Zhou J., Feng Y., Chen H. *J. Am. Chem. Soc.*, **140**, 15560 (2018).
57. Liu G., Liu Y., Liu X., Chen J., Fu G., Liu Z. *Sol. Energy Mater. Sol. Cells*, **186**, 142 (2018).
58. Lu X., Huang Y., Liu B., Zhang L., Song L., Zhang J., Zhang A., Chen T. *Chem. Mater.*, **30**, 1989 (2018).
59. Ma C., Gao Q., Hong W., Fan J., Fang J. *Adv. Funct. Mater.*, **27**, 1 (2016).
60. Nam J.-M., Oh J.-W., Lee H., Suh Y.D. *Acc. Chem. Res.*, **49**, 2746 (2016).
61. Pan R., Yang Y., Wang Y., Li S., Liu Z., Su Y., Quan B., Li Y., Gu C., Li J. *Nanoscale*, **10**, 3171 (2018).
62. Shin Y., Song J., Kim D., Kang T. *Adv. Mater.*, **27**, 4344 (2015).
63. Sigle D.O., Mertens J., Herrmann L.O., Bowman R.W., Ithurria S., Dubertret B., Shi Y., Yang H., Tserkezis C., Aizpurua J., Baumberg J.J. *ACS Nano*, **9**, 825 (2015).
64. Yoo D., Mohr D.A., Vidal-Codina F., John-Herpin A., Jo M., Kim S., Matson J., Caldwell J.D., Jeon H., Nguyen N.C., Martin-Moreno L., Peraire J., Altug H., Oh S.H. *Nano Lett.*, **18**, 1930 (2018).
65. Zhou J., Xiong Q., Ma J., Ren J., Messersmith P.B., Chen P., Duan H. *ACS Nano*, **10**, 11066 (2016).
66. Sarychev A.K., Ivanov A.V., Afanasyev K.N., Bykov I.V., Boginskaya I.A., Kurochkin I.N., Lagarkov A.N., Merzlikin A.M., Mikheev V.V., Negrov D.V., Ryzhikov I.A., Sedova M.V. *Quantum Electron.*, **48** (12), 1147 (2018) [*Kvantovaya Elektron.*, **48** (12), 1147 (2018)].
67. Sarychev A.K., Bykov I.V., Boginskaya I.A., Ivanov A.V., Kurochkin I.N., Lagarkov A.N., Nechaeva N.L., Ryzhikov I.A. *Opt. Quantum Electron.*, **52**, 26 (2019).
68. Johnson P.B., Christy R.W. *Phys. Rev. B*, **6**, 4370 (1972).